Lubrication of industrial contacts: accounting for roughness contribution with a reduced order model

J.-D. Wheeler[1], V. Bruyere[1], D. Dureisseix[2], N. Fillot[2], P. Namy[1], J. Raisin[3]
1. SIMTEC, 5 rue Félix Poulat, Grenoble, France
2. INSA Lyon, CNRS, LaMCoS, UMR5259, 69621 Villeurbanne, France
3. TotalEnergies OneTech, Solaize, France

Abstract
While the modelling of smooth concentrated contact lubrication has been achieved a few decades ago (1), the engineer is often left with no other option than to neglect many aspects of real-world contacts. Among these aspects, the contribution of roughness in lubricated contacts is computationally too expensive most of the time. However, a comprehensive homogenization method allows for the mathematical separation of the contact scale from the roughness microscale, enabling them to be solved in distinct domains in a fully coupled manner (2). This approach enables quantitative predictions in contrast to explicit solutions, but it remains computationally demanding. In this presentation, the authors demonstrate the feasibility of reducing the parametrization of roughness scale equations and interpolating their contribution using a method based on Gaussian Process Regressions. This method allows for solving the microscale contribution through pre-calculations and using them in a lubricated contact model. This is a proof of concept which establishes the feasibility of the method. It constitutes a milestone toward the resolution of rough contact lubrication within an industrially feasible timeframe.
Keywords: EHL, Multiscale, FE², Reduced order model, Gaussian Process Regression

Introduction
The size of typical concentrated contact (tens of µm to a few mm) is several orders of magnitude smaller than the device (from cm to several m) it serves. However, the contact performance over time is known to depend largely on surface microgeometry or surface roughness (3) (with roughness characteristic size between tens of nm to several µm). Experimental works are numerous, but models are still important to propose and verify explanations for the observed phenomena.
Including the microgeometry influence in the contact modeling constitutes a challenge and several approaches are developed in the literature depending on the end goal. Historically, *averaging methods* became available first thanks to their low computation cost; Patir & Cheng (4,5) seminal work is still used nowadays in the industry. Averaging methods rely on flow factors supposed to account for microgeometry influence, but the results mostly apply to a smooth equivalent contact and lack accuracy. It is however sufficient if qualitative results are deemed sufficient. A direct resolution of the contact equation up to the microscopic scale became available later in some cases with the advances of software and hardware capabilities. Such method is known as *deterministic approach* and a milestone in this regard is found in the work of Quiñonez *et al.* (6). Whereas software and hardware are still making regular progress, the deterministic approach is accessible for roughness not too small compared to the contact dimensions. Indeed, the discretization of the domain must be much smaller than the characteristic dimensions of the roughness, but the domain size is intimately related to the contact dimensions. Moreover, a fine discretization in time for transient problems makes the challenge even less accessible in many applications.

There is also a third way, stemming from *averaging methods* which are *homogenization methods*. While the former are based on relevant scientific intuition, the latter benefit from more formal mathematical developments. Bayada proposed a formal definition of flow factors (7) and Bayada *et al.* (8,9) computed the first homogenized results for concentrated contact at the cost of several simplifying assumptions. Budt *et al.* (10) included the deformation taking place at the local scale with a FE²-type method, with the roughness scale appearing as local extra-dimensions to the contact dimensions. Scaraggi *et al.* (11,12) considered finite-wavelength roughness but their approach is limited to low contact pressure with pressure independent lubricant properties. Checo *et al.* (2) proposed a homogenized model for the stationary elastohydrodynamic lubricated (EHL) line contact with pressure dependent lubricant viscosity and density. The equations are solved with a FE² approach. The surface roughness is of finite dimensions and thus the method they proposed does not depend on the limited case of infinitesimal roughness size. While this last work is a breakthrough, the computation effort that comes with FE² method forbids its usage for the transient case or the point contact: it appears necessary to compute the microgeometry behavior more efficiently.
This work proposes a method to solve microgeometry equations prior to the full contact

computation, and to summarize their response in a reduced order model (ROM). First, classical EHL equations are reminded to the reader. Then the multiscale EHL equations are presented before detailing the flow factors that are later summarized in the ROM. At last, results using this method are presented.

Classical EHL equations

EHL occurs at the conjunction between two convex bodies with fluid entrainment capacity as seen in Figure 1a. In this picture, the bodies are assumed to have an infinite out of plane length with an evenly distributed load w: it is a line contact, as opposed to the more general point contact. The entrainment capacity is summarized by $u_e = (u_t + u_b)/2$ the entrainment velocity, with u_t the velocity of the top body surface and u_b the velocity at the bottom body surface. At this stage, perfectly smooth surfaces are assumed.

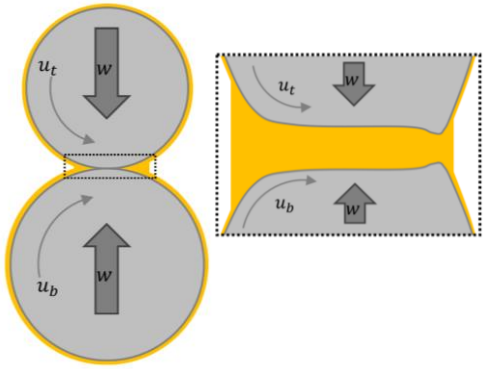

Figure 1: a) Two bodies with EHL occurring at the conjunction (left), b) zoom at the conjunction between the two bodies (right).

While focusing its attention on the conjunction in Figure 1b, the reader notices (1) the full separation of the solids by the fluid, (2) the local specific shape of the solids which is due to specific hydrodynamic pressure distribution and (3) a meniscus which concentrates the fluid at the contact vicinity.

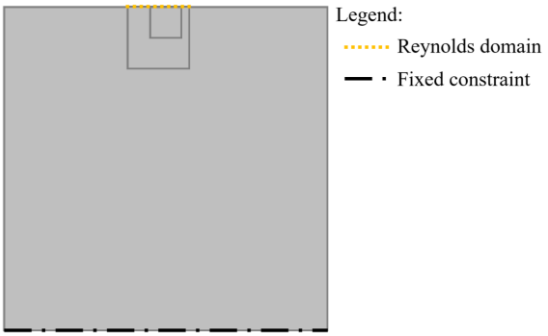

Figure 2: EHL computation domains at the contact scale.

EHL computation using COMSOL Multiphysics dates back to the developments of Habchi *et al.* (13) and it is this paper that inspires the present EHL implementation. The equation set are presented in their dimensional form, but the dimensionless versions allow for using unit size geometries as computation domain (see Figure 2 and Figure 3).

Reynolds equation

A lower dimension Navier-Stokes equation is used to compute the thin film, namely the Reynolds equation:

$$\frac{\partial}{\partial x}\left(\frac{\rho h^3}{12\eta}\frac{\partial p}{\partial x}\right) - u_e\frac{\partial}{\partial x}(\rho h) - \frac{\partial}{\partial t}(\rho h) = 0$$

with ρ the fluid density, η its viscosity, x the position in the contact along contact entrainment direction, u_e the entrainment velocity, h the film thickness and p the pressure which is also the variable solved for here. This equation is solved on the dotted line domain Ω in Figure 2, and the boundaries of this line are attributed a $p = 0$ Dirichlet boundary condition.

Solid linear elasticity

The hydrodynamic pressure computed is applied as a boundary load to a single solid domain (in grey in Figure 2) which elastic properties are equivalent to the cumulated behavior of the two bodies (14). A fixed constraint is applied at the bottom of this solid. Computing the elastic deformation provides the local elastic deformation sum v which feeds the film thickness expression:

$$h = h_0 + \frac{x^2}{R_x} + v$$

with R_x the reduced curvature radius of the two bodies and h_0 the rigid body distance.

Load balance

This rigid body distance is a scalar which defines the solid separation capability of the fluid and is defined by solving the load balance equation:

$$w = \int_{\Omega} p\, dx$$

Although not appearing explicitly in this equation, h_0 value is successfully obtained by computing the full equation system (*ie.* Reynolds equation, solid linear elasticity and load balance) in a fully coupled manner.

Multiscale EHL equations

For engineering purposes, one can consider multiscale introduction in the EHL equation by two main ideas:

- Classical space dimension x is now instead defined by $\breve{x}$ the dimension at the contact scale and $\tilde{x}$ is the dimension at the roughness scale. The breve $\breve{\square}$ denotes contact variables in the followings, and the tilde $\tilde{\square}$ denotes the roughness variables. A scale factor $\varepsilon = \lambda / b$ separates the two dimensions, with λ the roughness wavelength and b the Hertzian contact semi-width. The classical $\partial\cdot/\partial x$ derivation operator is replaced by $\partial\cdot/\partial\breve{x} + {}^1/_{\varepsilon}\ \partial\cdot/\partial\tilde{x}$ which can be assimilated to a multiscale derivation operator. Since fast variations occur due to roughness motion

time derivation is redefined with $\partial\cdot/\partial\check{t} + {}^{1}/_{\varepsilon}\ \partial\cdot/\partial\tilde{t}$ using the same scale factor.
- The problem unknowns are developed with respect to this scale factor ε. For the pressure it reads: $p = \varepsilon^0\check{p} + \varepsilon^1\tilde{p} + \cdots$.

Thanks to the two notions presented, the classical EHL equations show terms of different ε orders and the following equation system is defined.

Roughness scale Reynolds equation

An equation very similar to Reynolds equation can be identified within the ε^{-1} terms:

$$\frac{\partial}{\partial\tilde{x}}\left(\frac{\rho h^3}{12\eta}\left(\frac{\partial\tilde{p}}{\partial\tilde{x}}+\frac{\partial\check{p}}{\partial\check{x}}\right)\right) - u_e\frac{\partial}{\partial\tilde{x}}(\rho\tilde{h}) - \frac{\partial}{\partial\tilde{t}}(\rho\tilde{h}) = 0$$

with $h = \check{h}(\check{x}) + \tilde{h}(\check{x},\tilde{x})$ the complete film gap, $\check{h}$ the contact scale film thickness (defined precisely later), $\tilde{h} = 0 + \widetilde{h_r} + \varepsilon\,\tilde{v}$ the film thickness fluctuation, $\widetilde{h_r}$ the rigid surface roughness gap and $\tilde{v}$ the roughness scale deformation sum. Both last terms verify a zero sum across $\widetilde{\Omega}$. Since most terms of the above-described equation are defined using roughness scale variables, it is called the Reynold roughness scale equation. The $\partial\check{p}\ /\ \partial\check{x}$ term is an exception, and it behaves like a pressure gradient source term coming from contact scale. This equation is solved along the boundary represented in Figure 3, with periodic boundary condition on pressure $\tilde{p}$. The transient roughness scale computation also requires time-periodic boundary conditions: there are different ways to achieve such boundaries, but the method selected consists in computing many cycles and stop once the time-periodic steady state is attained, thus realizing time-periodic boundary conditions.

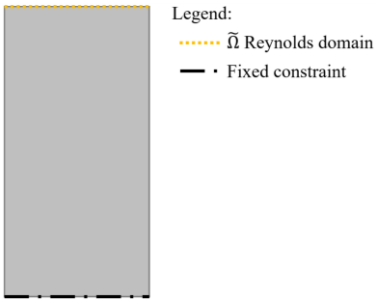

Figure 3: Roughness scale computation domains.

To isolate the behavior of the fluid and the surface microgeometry in response to the different source terms, different reduced versions of the roughness scale Reynolds equation are also solved:

$$\frac{\partial}{\partial\tilde{x}}\left(\frac{\rho h^3}{12\eta}\frac{\partial\widetilde{p_1}}{\partial\tilde{x}}\right) - u_e\frac{\partial}{\partial\tilde{x}}(\rho\tilde{h}) - \frac{\partial}{\partial\tilde{t}}(\rho\tilde{h}) = 0$$

$$\frac{\partial}{\partial\tilde{x}}\left(\frac{\rho h^3}{12\eta}\left(\frac{\partial\widetilde{p_2}}{\partial\tilde{x}}+\frac{\partial\check{p}}{\partial\check{x}}\right)\right) - \frac{\partial}{\partial\tilde{t}}(\rho\tilde{h}) = 0$$

$$\frac{\partial}{\partial\tilde{x}}\left(\frac{\rho h^3}{12\eta}\frac{\partial\widetilde{p_3}}{\partial\tilde{x}}\right) - \frac{\partial}{\partial\tilde{t}}(\rho\tilde{h}) = 0$$

respectively for pressure fluctuation alternative variables $\widetilde{p_1}$, $\widetilde{p_2}$, and $\widetilde{p_3}$. $\widetilde{p_1}$ equation omits the contact scale pressure gradient source term, $\widetilde{p_2}$ equation omits the Couette source term, and $\widetilde{p_3}$ equation omits both the contact scale pressure gradient source term and Couette source term. It is worth noting that all 3 additional equations are solved for the film thickness (and deformation) under the load of $\tilde{p}$, and not the load of the alternative variable. One can show that $\tilde{p} = \widetilde{p_1} + \widetilde{p_2} - \widetilde{p_3}$ which comes in use for later flow factor computation.

Roughness scale load balance

The previously defined roughness scale Reynolds equation provides a solution of $\tilde{p}$ up to an additive constant. The unicity of the equation system is obtained by selecting the solution verifying $\int_{\widetilde{\Omega}}\tilde{p}\ d\tilde{x} = 0$. Indeed, $\tilde{p}$ constitutes a fluctuation of the pressure due to the roughness, and it fluctuates around the contact pressure $\check{p}$ which also becomes a mean pressure. This contact pressure is computed in the contact scale Reynolds equation and the classical EHL load balance.

Roughness scale linear elasticity

The solid deformation at the roughness scale is computed with linear elasticity equation. The pressure fluctuation $\tilde{p}$ is applied as a load at the top of the solid as seen in Figure 3, and a fixed constraint is applied at the bottom. The two remaining boundaries verify periodic boundary condition on solid displacement.

Contact scale Reynolds equation

Thanks to the formal homogenization development, additional terms emerge in a contact scale Reynolds equation. Such terms are best known in the literature as flow factors and their specific nature will be detailed in the next section. This contact scale equation is composed of the of ε^0 terms and reads:

$$\frac{\partial}{\partial\check{x}}\left(\frac{\check{\rho}\check{h}^3}{12\check{\eta}}\Phi_x\frac{\partial\check{p}}{\partial\check{x}}\right) = u_e\frac{\partial}{\partial\check{x}}(\check{\rho}\Phi_s\check{h}) + \frac{\partial}{\partial\check{t}}(\check{\rho}\check{h}) + r$$

with Φ_x and Φ_s classical flow factors, r a new flow factor emerging from the homogenization procedure, $\check{\rho}$ and $\check{\eta}$ respectively the density and viscosity of the fluid only depending on the contact scale pressure $\check{p}$, and $\check{h} = h_0 + \check{x}/R_x^2 + \check{v}$ expressed similarly to the classical film thickness expression.

While Checo *et al.* (2) solved this whole multiscale equation set in a fully coupled manner, the presence of the flow factor terms and the existence of a rigorous mathematical definition, open the possibility to compute them once and for all separately.

Flow factors and relocation

The flow factors depend on only three macroscopic variables $\check{h}$, $\check{p}$ and $\partial\check{p}\ /\ \partial\check{x}$. In response, they provide the contact scale Reynolds equation with ponderations which translate the microgeometry effects on the flow at the contact scale.

Poiseuille flow factor

The first flow factor, Φ_x, is obtained with the average expression:

$$\Phi_x = \frac{1}{\lambda}\int_{\tilde{\Omega}} \left(\frac{\rho h^3}{12\eta} \cdot \frac{12\check{\eta}}{\check{\rho}\check{h}^3} \cdot \left(1 - \frac{\frac{\partial \widetilde{p_3}}{\partial \tilde{x}} - \frac{\partial \widetilde{p_2}}{\partial \tilde{x}}}{\frac{\partial \check{p}}{\partial \tilde{x}}} \right) \right) dx$$

Couette flow factor

The second flow factor, Φ_s, is obtained similarly with the average expression:

$$\Phi_s = \frac{1}{\lambda}\int_{\tilde{\Omega}} \frac{1}{\check{\rho}\check{h}} \left(\rho h - \frac{\rho h^3}{12\eta} \left(\frac{\partial \widetilde{p_1}}{\partial \tilde{x}} - \frac{\partial \widetilde{p_3}}{\partial \tilde{x}} \right) \right) dx$$

Transient flow factor

At last, r is defined by:

$$r = \frac{\partial}{\partial \tilde{x}} \left(\frac{1}{\lambda}\int_{\tilde{\Omega}} \left(\frac{\rho h^3}{12\eta} \cdot \frac{\partial \widetilde{p_3}}{\partial \tilde{x}} \right) dx \right)$$

For the sake of practicality, the ROM for this transient flow factor is built on $\log_{10}\left(\int r\, dx\right)$ and it is only in the contact model that r is computed.

Relocation

The final goals of such modelling method are:

1. To predict quantitatively the contact behavior with microgeometry influence,
2. And to predict the minimum film thickness and maximum pressure peaks due to the microgeometry with the account of local deformation.

The latter goal is called relocation, and it requires supplementary information from the roughness scale computation. The complete profile of the pressure and film thickness fluctuations are computed in the simulation, but the minima and maxima of the profiles are sufficient to meet goal n°2. These minima and maxima are called relocation variables.

Reduced order model

Parametrization, scaling and thresholds

Since the flow factors depend only on the macroscopic variables $\check{h}$, $\check{p}$ and $\partial\check{p}\,/\,\partial\check{x}$, it is possible to define a virtual 3-dimensional space based on them. However, their influence on the flow factors is not necessarily linear. In the following, this space is mapped using $H = \log_{10}\left(\check{h}R_x\,/\,b^2\right)$, $P = \log_{10}(\check{p})$ and $Z = (b\,/\,p_h)\cdot\partial\check{p}\,/\,\partial\check{x}$ respectively (with p_h the contact Hertzian pressure).

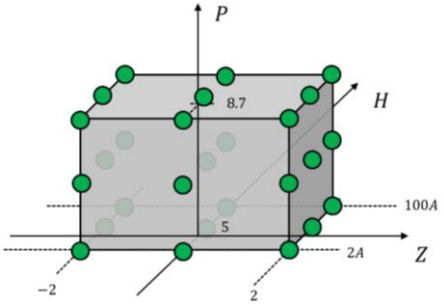

Figure 4: Cuboid and its training sites.

Any geometrical point located on the Reynolds domain (i.e. in the contact or its vicinity) has a film thickness, a pressure and a pressure gradient which define a position in this virtual space. However, the realistic operating condition of a real world EHL contact are limited, which translated in the H, P, Z space defines a restricted region. Moreover, the H, P, Z conditions that significantly contribute to defining the film build-up and determine lubrication are even more restricted. It is therefore possible to target the relevant positions in the virtual space and only focus on those. These relevant positions are bound within a cuboid of the virtual space (represented in Figure 4):

- $\log_{10}(2A) \leq H \leq \log_{10}(100A)$ where A is the dimensionless roughness amplitude. The lower boundary is before the boundary regime, whereas the upper boundary represents a film thickness at which roughness is not supposed to contribute to the flow,
- $5 \leq P \leq 8.7$ which corresponds to the range between ambient pressure and $500MPa$; for the considered lubricant, the flow is considered as almost zero above this threshold,
- $-2 \leq Z \leq 2$ which is a reasonable bounding of the range of pressure gradients occurring at the contact inlet, during film build-up.

The validity of the ROM is limited to a roughness-lubricant couple. Any change of roughness or lubricant requires a new ROM.

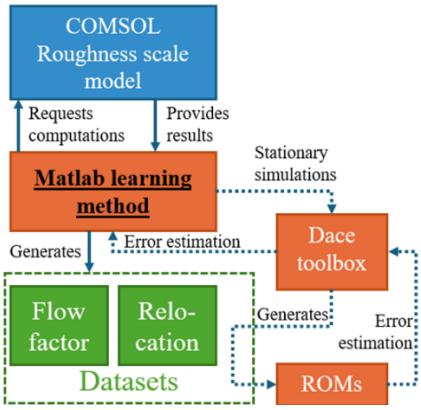

Figure 5: roughness scale learning algorithms (solid arrows: all simulations, dotted arrow: stationary simulations only, Underlined black & bold text: main method)

Kriging with Dace or classical interpolation

COMSOL alone cannot run an algorithm to build the desired ROM, but its coupling capabilities with MATLAB allow for using additional tools:

- For the stationary version of the multiscale EHL model, the Dace MATLAB toolbox (15) is selected.
- For the transient version of the multiscale EHL model, an interpolation using the classical *interp3* MATLAB function is selected.

The Dace toolbox contains training tools to build a ROM and tools to answer queries efficiently on the ROM. The method used by Dace is a type of

Gaussian Process Regression. Dace MATLAB toolbox answers the exact training value to queries targeted on its training sites and can interpolate between the training sites in spaces of any dimensions (even though the dimension is only 3 here).

Algorithm

The cuboid defined in Figure 4 is mapped with 27 training sites. For each site, the MATLAB learning method requests a computation at the COMSOL roughness scale model (see Figure 5) and the Φ_x, Φ_s, and r flow factors are evaluated together with the relocation variables.

For the stationary simulations, many test sites (e.g. 10^5) are also defined using a Latin hypercube distribution in the cuboid. After training the Dace ROMs on the 27 first sites, the Dace toolbox (see Figure 5, with dotted arrows) can quickly answer the 10^5 queries together with an estimate of the error on each test sites. The test site with the largest error can be used to start a new COMSOL roughness scale model (see Figure 5) computation, and the new result can be used as an additional training site for the ROMs. After the model is updated, the $10^5 - 1$ remaining testing sites can be used to assess the updated ROM errors again. This process of training-testing-improving can be repeated until the maximum error reaches a specific threshold or after a pre-defined number of iterations. During the COMSOL Contact scale model (see Figure 6Figure 5) computation, each flow factor is determined by calling a MATLAB function (see Figure 6) which loads the relevant ROM and assesses the flow factor space-dependent vector in response to the space-dependent vectors of H, P and Z. During post-treatment, the same process is applied to determine the lower and upper values of both film thickness and pressure by calling the relocation ROMs.

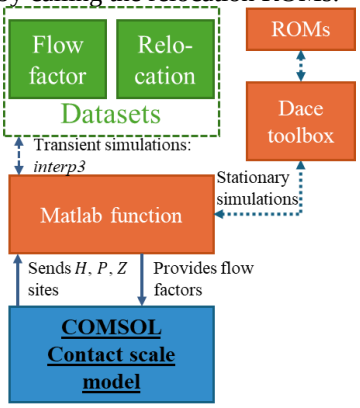

Figure 6: Contact scale computation algorithm (solid arrows: all simulations, dotted arrow: stationary simulations only, dashed arrow: transient only, Underlined black & bold text: main method)

For the transient simulations, only the 27 first training sites are used. No ROM is built. During COMSOL Contact scale model computation, each flow factor is determined by calling a MATLAB function (see Figure 6) which uses the *interp3* MATLAB function exploiting the 27 training sites. The *interp3 linear* interpolation is used for the relocation variables, Φ_x and Φ_s, but the more advanced *maxima* interpolation allows for handling the transient flow factor. During post-treatment, the same process is applied to determine the lower and upper values of both film thickness and pressure by interpolation on the relocation datasets.

The limited number of training sites in the transient computation is due to the large computation time required: the 27 training computations need approximately 70h on a 3.5GHz 4 cores processor. Since the interpolations built with such limited data provided satisfactory performance for a proof-of-concept, the Dace library and training-testing-improving process was not used in the transient computation presented in the result section.

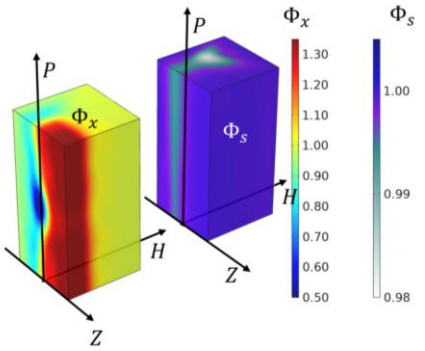

Figure 7: Stationary simulation flow factor representations (600 training sites and 10^5 testing sites)

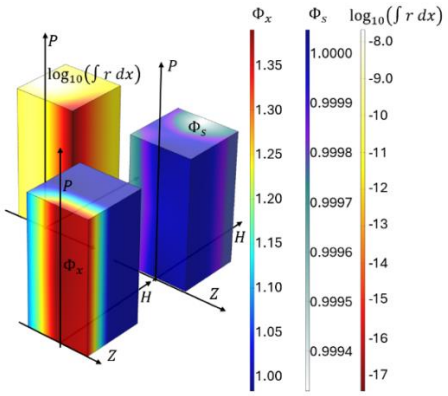

Figure 8: Transient simulation flow factor representations (27 computed sites only)

Results

The stationary results presented in the followings correspond to a $M = 100$ and $L = 5.3$ case using Moes parameters. The computation is run with $R_x = 1.344\,mm$, $w = 154\,kN/m$, $u_e = 1\,m/s$, which results in $p_h = 2\,GPa$, $b = 49\,\mu m$ and $h_{min} = 14\,nm$. A roughness of amplitude $A = 1.4\,nm$ is studied, with a wavelength of $\lambda = 4.9\,\mu m$.

The transient results presented in the followings correspond to a $M = 31.6$ and $L = 2.4$ case using Moes parameters. The computation is run with $R_x = 344\,mm$, $w = 2460\,kN/m$, $u_e = 10\,m/s$, which

results in $p_h = 0.5\,GPa$, $b = 3.1\,mm$ and $h_{min} = 596\,nm$. A roughness of amplitude $A = 60\,nm$ is studied, with a wavelength of $\lambda = 0.31\,mm$. The contact covers a $8 \cdot b$ amplitude reciprocal linear motion, following a sine velocity pattern.

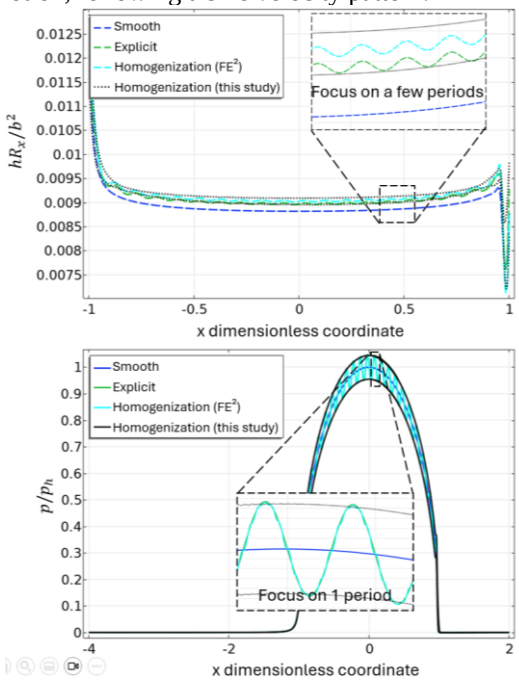

Figure 9: Comparison of different approaches to the computation of rough contacts: smooth assumption, explicit method, homogenization (FE²) and homogenization (this study). Top: film thickness, bottom: pressure

Flow factors

In the stationary computation, only two flow factors are required. They are represented in Figure 7. The Poiseuille flow factor $0.50 < \Phi_x < 1.35$ shows a range which can sensibly influence the Reynolds equation diffusion coefficient depending on the H, P, Z triplet. The Couette flow factor has a more limited range.

The three transient flow factors obtained by interpolation are represented in Figure 8. Whereas the Poiseuille flow factor $0.95 < \Phi_x < 1.4$ shows a more limited range compared to the stationary equivalent, Φ_s shows an even more restricted range and is almost always equal to 1. Finally, the transient flow factor is poor in meaning under this shape.

The differences in amplitude between the stationary and transient Φ_x and Φ_s flow factors may be due to the limited number of sites used for the transient ones. Indeed, the lack of sites can lead to avoiding the more extreme values in the H, P, Z cuboid. This difference also advocates for the use of a proper training-testing-improving routine.

Contact scale stationary results

The contact scale stationary case film thickness and pressure results are presented in Figure 9. Different approaches to rough contact modelling are compared. The smooth contact assumption leads to underestimate the maximum pressure and the average film thickness value computed with the explicit approach (which is computationally affordable here and serves as a reference). The homogenization (FE²) approach shows a good prediction of both film thickness and pressure computed with the explicit approach. Finally, the homogenization method presented in this study shows a very accurate prediction of the envelope of pressures and a good prediction of average film thickness. However, it tends to overestimate the amplitude of the film thickness fluctuations. This is probably due to the training sites which are limited at $0.5\,GPa$ maximum pressure, whereas the contact experiences $2\,GPa$ maximum pressure and thus more roughness deformation.

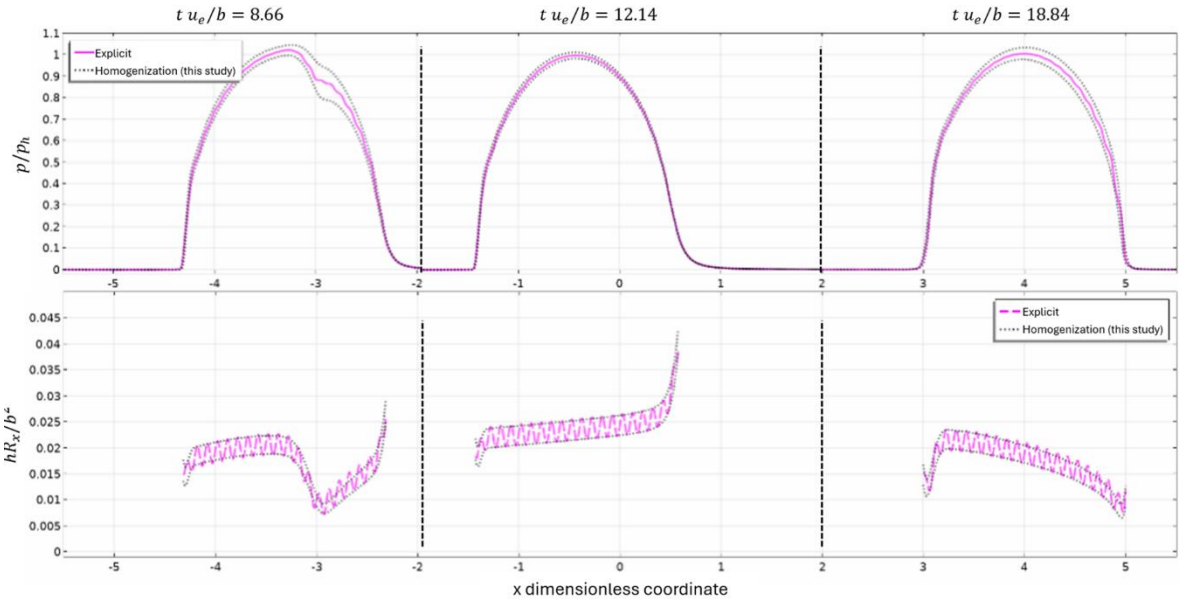

Figure 10: Contact scale transient results at different times. Comparison between explicit and homogenization (this study), Top: pressure, bottom: film thickness

Contact scale transient results

Even though the flow factors may lack accuracy over the range of the cuboid, they are used to run a transient simulation. The explicit (computationally affordable, with 42 min computation on a 3.5GHz 4 cores processor) and homogenization (this study, 30 min computation on the same computer) methods are compared at different dimensionless times in Figure 10. The pressure behavior at contact scale is well predicted by the homogenization method, but the pressure fluctuation amplitude is overestimated. Both contact scale and roughness scale film thickness are well predicted by the homogenization method. The computation time is similar for both methods, but much smaller roughness would make the explicit computation unaffordable whilst the homogenization method computation time unaffected.

Conclusions

A homogenization method for the study of rough contact is presented in this document. The method consists in decoupling the contact and roughness scales. Through a formal mathematical procedure, it is possible to compute the roughness lubrication behavior independently and prior to the contact scale computation. The accuracy of the homogenization method results was satisfactory in the stationary and transient cases, but the limited range of operating condition tested calls for further investigations. Moreover, the computation time of the transient flow factors and relocation variables requires further work to become more affordable.

References

1. Hamrock BJ, Dowson D. Isothermal elastohydrodynamic lubrication of point contacts - Part 1 to 4. J Lubr Technol. 1977;
2. Checo HM, Dureisseix D, Fillot N, Raisin J. A homogenized micro-elastohydrodynamic lubrication model: Accounting for non-negligible microscopic quantities. Tribol Int. 2019;135:344–54.
3. Morales-Espejel GE, Brizmer V. Micropitting modelling in rolling–sliding contacts: Application to rolling bearings. Tribol Trans. 2011;54(4):625–43.
4. Patir N, Cheng HS. Application of average flow model to lubrication between rough sliding surfaces. J Tribol. 1979;101(2):220–9.
5. Patir N, Cheng HS. An average flow model for determining effects of three-dimensional roughness on partial hydrodynamic lubrication. 1977;100(January):12–7.
6. Félix-Quiñonez A, Ehret P, Summers JL. On three-dimensional flat-top defects passing through an EHL point contact: A comparison of modeling with experiments. J Tribol. 2005 Jan;127(1):51–60.
7. Bayada G. Application of the homogenization method to Reynolds roughness. In: Developments in Numerical and Experimental Methods Applied to Tribology [Internet]. Lyon, France: Elsevier; 1984. p. 53–9. Available from: https://linkinghub.elsevier.com/retrieve/pii/B9780408221641500119
8. Bayada G, Martin S, Vázquez C. Homogenization of a nonlocal elastohydrodynamic lubrication problem: a new free boundary model. Math Model Methods Appl Sci [Internet]. 2005 Dec 21;15(12):1923–56. Available from: https://www.worldscientific.com/doi/10.1142/S0218202505001023
9. Bayada G, Martin S, Vázquez C. Micro-roughness effects in (elasto)hydrodynamic lubrication including a mass-flow preserving cavitation model. Tribol Int [Internet]. 2006 Dec;39(12):1707–18. Available from: https://linkinghub.elsevier.com/retrieve/pii/S0301679X06001757
10. Budt M, Temizer İ, Wriggers P. A computational homogenization framework for soft elastohydrodynamic lubrication. Comput Mech [Internet]. 2012 Jun 28;49(6):749–67. Available from: http://link.springer.com/10.1007/s00466-012-0709-7
11. Scaraggi M, Carbone G, Dini D. Lubrication in soft rough contacts: A novel homogenized approach. Part II - Discussion. Soft Matter [Internet]. 2011;7(21):10407. Available from: https://xlink.rsc.org/?DOI=c1sm05129f
12. Scaraggi M, Dorogin L, Angerhausen J, Murrenhoff H, Persson BNJ. Elastohydrodynamics for Soft Solids with Surface Roughness: Transient Effects. Tribol Lett [Internet]. 2017 Sep 9;65(3):95. Available from: http://link.springer.com/10.1007/s11249-017-0878-9
13. Habchi W, Eyheramendy D, Vergne P, Morales-Espejel GE. A full-system approach to the elastohydrodynamic line/point contact problem. J Tribol. 2008;130(2):21501–10.
14. Habchi W. A full-system finite element approach to elastohydrodynamic lubrication problems: application to ultra-low-viscosity fluids [Internet]. INSA; 2008. Available from: https://theses.fr/2008ISAL0038
15. Lophaven SN, Nielsen HB, Sondergaard J. DACE - A Matlab Kriging Toolbox [Internet]. 2002. Available from: https://www.omicron.dk/dace.html